Alternative antigen processing and presentation pathways by tumors

Cunha, Oliveira C. da

3

NEW ROLE OF SIGNAL PEPTIDE PEPTIDASE TO LIBERATE C-TERMINAL PEPTIDES FOR MHC CLASS-I PRESENTATION

Cláudia C. Oliveira[1,4], Bianca Querido[1], Marjolein Sluijter[1], Anne F. de Groot[1], Reno van der Zee[1], Martijn J.W.E. Rabelink[2], Rob C. Hoeben[2], Ferry Ossendorp[3], Sjoerd H. van der Burg[1] and Thorbald van Hall[1]

[1]Department of Clinical Oncology,
[2]Department of Molecular Cell Biology
and [3]Department of Immunohematology and Blood Transfusion,
Leiden University Medical Center, Leiden, the Netherlands;
[4]Graduate Program in Areas of Basic and Applied Biology,
Porto, Portugal.

Accepted for publication in: *Journal of Immunology*

| ABSTRACT

The signal peptide peptidase (SPP) is an intra-membrane cleaving aspartyl protease involved in release of leader peptide remnants from the ER membrane, hence its name. We now found a new activity of SPP that mediates liberation of C-terminal peptides. In our search for novel proteolytic enzymes involved in major histocompatibility complex class I (MHC-I) presentation, we found that SPP generates the C-terminal peptide-epitope of a ceramide synthase. The display of this immunogenic peptide/MHC-I complex at the cell surface was independent of conventional processing components like proteasome and peptide transporter TAP. Absence of TAP activity even increased the MHC-I presentation of this antigen. Mutagenesis studies revealed the crucial role of the C-terminal location of the epitope and 'helix-breaking' residues in the transmembrane region just upstream of the peptide, indicating that SPP directly liberated the minimal 9-mer peptide. Moreover, silencing of SPP and its family member SPPL2a led to a general reduction of surface peptide/MHC-I complexes, underlining the involvement of these enzymes in antigen processing and presentation.

| INTRODUCTION

All nucleated cells of our body display a representative selection of the cellular proteome in Major Histocompatibility class I (MHC-I) molecules at their surfaces. This wide array of peptides serves as ligands for $CD8^+$ T-cells for cellular immunity. The process of peptide presentation starts with the proteolysis of aged or misfolded proteins, a process mainly executed by the multi-catalytic action of proteasomes. The generated peptide sequences are translocated from the cytosol into the ER by the TAP peptide transporters, where they are assembled with different MHC-I molecules with help from members of the peptide loading complex, including calreticulin, tapasin and ERp57. Stable peptide/MHC-I complexes are routed to the cell surface. This proteasome-TAP pathway is considered as the conventional processing route, used to generate and shuttle the majority of peptides[1-3]. Additional players, like tripeptidyl peptidase II (TPPII) and nardilysin are responsible to further shorten proteasomal intermediates or, sometimes, to directly generate minimal peptide sequences that fit in MHC-I molecules[4, 5].

Although these central elements of the conventional antigen processing pathway are important for the mainstream of peptides, substantial MHC-I antigen presentation is still detectable on cells in which the function of key components is compromised. For example, deficiency in the peptide transporter TAP, which can be regarded as a bottleneck in the pathway, results in a decreased surface MHC-I, but the residual peptide repertoire is sufficient to generate a diverse $CD8^+$ T cell subset in mice[6-8] and man[9, 10]. Importantly, this T cell repertoire is capable to control common viral infections and from some TAP-deficient patients $TCR\alpha\beta^+$ $CD8^+$ T-cell clones were isolated that recognized TAP-independent viral antigens[11, 12]. Therefore, TAP-independent processing pathways may sufficiently compensate for the loss of the conventional route in order to select a functional $CD8^+$ T-cell repertoire in these patients.

This reasoning is in line with our recent findings on a novel category of T cell epitopes presented by cancer cells with TAP-defects. We showed that deficiency in the expression of the peptide transporter TAP, a feature frequently found in human cancers, leads to the presentation of a broad repertoire of immunogenic peptides by MHC-I[13-17]. Biochemical characterization of peptide repertoires from TAP-deficient cells and their direct proficient counterparts indeed revealed unique complementing pools of peptides[14, 18, 19].

Two pathways for TAP-independent peptide loading are described thus far[20]. One of these is active in the secretory route of the Golgi and is mediated by the protein convertase furin[21-23]. The other concerns N-terminal leader sequences, which are liberated after arrival in the ER by the signal peptidase (SP). Cleavage by SP leaves small transmembrane leader peptide remnants in the ER membrane, which are removed by the intramembrane-cleaving signal peptide peptidase (SPP). The ER-directing parts of these peptides end up in the lumen of the ER and can be loaded unto MHC-I molecules[24, 25]. An immunogenic human tumor antigen from the leader sequence of calcitonin is released by this means and TAP is dispensable for its presentation on cancer cell lines[26, 27].

In the current study we reveal the processing pathway of a C-terminal peptide from the ceramide synthase Trh4 (also known as CerS5). This protein resides in ER membranes and docks its C-terminal epitope-containing tail into the bilayer. Intramembrane proteolysis by SPP just in front of the epitope resulted in liberation and TAP-independent loading on D^b molecules. This represents a novel role for SPP, acting independently from the signal peptidase (SP). Our data indicate that SPP is able to directly liberate minimal peptide-epitopes from the C-terminus of proteins by intramembrane proteolysis and underlines the involvement of this enzyme in antigen processing.

| RESULTS

The TAP-independent processing pathway of the Trh4-derived peptide is common and conserved

The Trh4-derived peptide MCLRMTAVM is presented by the MHC class I molecule H-2D^b on TAP-deficient tumor cells[17]. We were interested in the nature of its TAP-independent processing pathway that leads to the generation and surface presentation of the Trh4 peptide in D^b, and therefore, analyzed the generality of this antigen processing pathway in different mouse and human tumor cell lines (Fig 1). Four mouse tumor cell lines of different origin and containing a TAP defect (a lymphoma, a fibrosarcoma, a colon carcinoma and a melanoma) were analyzed for recognition by a previously established MCLRMTAVM-specific $CD8^+$ T-cell clone. These T cells efficiently recognized all TAP-deficient tumors, irrespective of their tissue origin (Fig 1A). Importantly, the different mechanisms underlying the TAP impediment in these tumors, being TAP2 mutation (in RMA-S), TAP1 gene loss (in MCA), expression of a small viral inhibitor (in MC38) or TAP2 gene loss (in B78H1), all led to efficient presentation of the Trh4-derived peptide, indicating that presentation of the Trh4 peptide is related to TAP-deficiency as such and not to a specific molecular mechanism. The fact that TAP-positive counterpart tumors presented much lower Trh4 peptide at their cell surface was not surprising, since we previously showed that restoration of TAP function decreases Trh4/D^b complexes at the cell surface, most likely due to competition[28]. Therefore, the Trh4 peptide presentation is TAP-independent and operates in different tumor types.

The degree of CTL recognition of the tumor cell lines varied and we wondered if these differences could be explained by Trh4 expression levels. Trh4 transcripts were quantified by qPCR and indeed revealed higher expression in the lymphoma RMA-S compared to the solid tumors (Fig 1B). Expression of a splice variant of Trh4, which does not contain the D^b-binding peptide, showed less variety in the tumor panel. We concluded that surface display of Trh4/D^b complexes is determined by TAP function, Trh4 protein levels and possibly other factors like the protease responsible for peptide liberation.

We also wanted to know if human cells were equipped with the TAP-independent processing pathway. The mouse Trh4 gene was introduced into the human cell lines HeLa and HEK293T, together with the mouse MHC class I gene H-2D^b that presents

this peptide. The Trh4-derived peptide was efficiently presented at the cell surface of both human lines, indicating that the involved processing pathway was indeed also active in human cells (Fig 1C). Although these human cells have intact TAP function and thereby impede Trh4 peptide presentation, the high expression levels of Trh4 protein, from strong heterologous promoters overcomes the competition of peptides from the proteasome-TAP pathway, as illustrated by efficient CTL recognition of TAP-positive RMA lymphoma cells in which Trh4 is expressed eight hundred times higher than the endogenous level[28]. Together, these data show that the TAP-independent processing

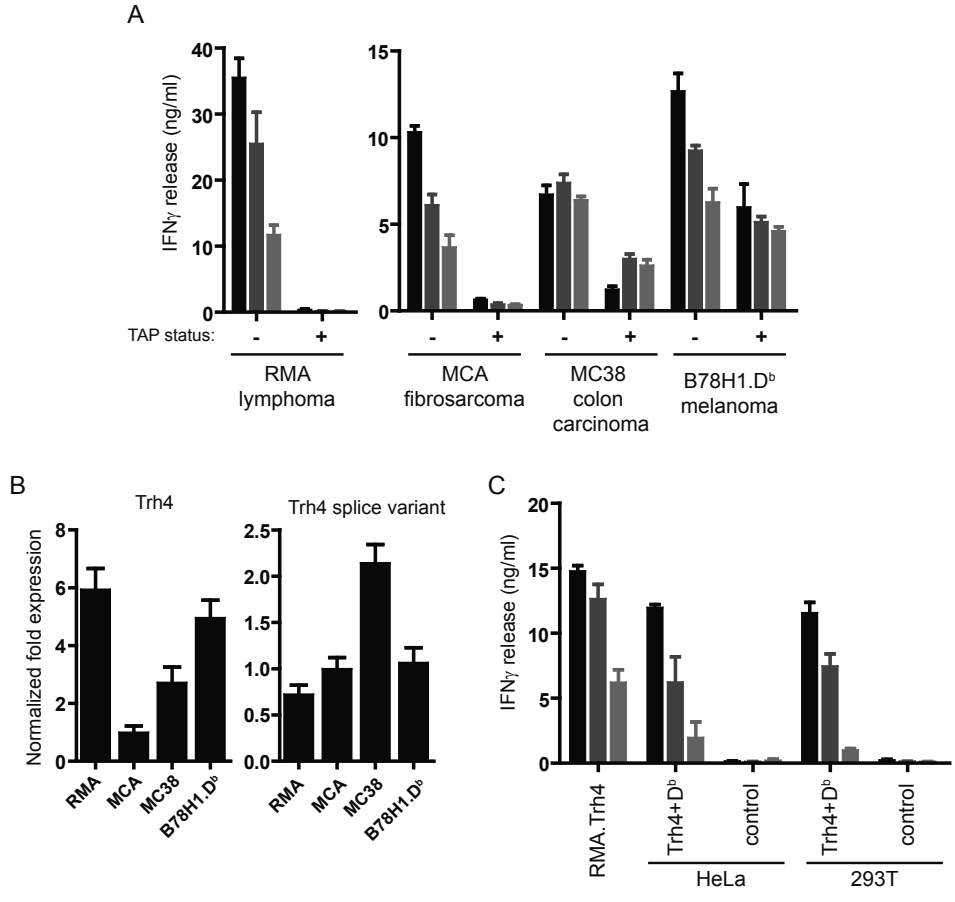

Figure 1. The Trh4 processing pathway is conserved and broadly active. (A) Presentation of Trh4-derived peptide by MHC-I was evaluated on lymphoma (RMA), fibrosarcoma (MCA), colon carcinoma (MC38) and melanoma cells (B78H1.D^b). Activation of Trh4-specific T cells is enhanced by the absence on peptide transporter TAP. (B) mRNA expression of Trh4 and a natural Trh4 splice variant was determined by quantitative PCR. The splice variant does not encode the Th4 peptide sequence due to a frame-shift. One out of three comparable experiments is shown. (C) Human 293T and HeLa cells were transfected with mouse Trh4 and H-2D^b genes and used as targets. Mean and standard deviation of triplicates are shown from one out of three experiments.

pathway that generates the Trh4 peptide is a common and conserved mechanism operational in mouse and human tumor cell lines of different histological origins.

The Trh4 protein is localized in the membrane of the endoplasmic reticulum

To unravel the processing pathway of the Trh4-derived peptide, we next determined the cellular localization the Trh4 protein. The Trh4 protein (also known as CerS5) belongs to a family of ceramide synthases (CerS1 to CerS6) and exists in two isoforms as a result of alternative splicing of the transcript[17]. The shorter protein variant (UniProt Q9D6K9-2) contains the D^b-presented peptide MCLRMTAVM at the complete end of its C-terminus. The longer protein (UniProt Q9D6K9-1) lacks this peptide sequence due to a frame shift at the last intron-exon boundary[17]. Although the longer isoform was described to be a multi-transmembrane spanning protein in the endoplasmic reticulum[32], no data were available concerning the Trh4 variant comprising the peptide-epitope. Algorithm programs predicting topology of transmembrane proteins anticipated that the short Trh4 protein would transgress membranes seven times with the C-terminal amino acids 373-384 located within the lipid bilayer, directed towards the lumen (Fig 2A). The V5 antibody epitope was introduced at two distinct sites of Trh4 gene constructs (C-terminal after the epitope and N-terminal at amino acid 32) and subcellular localization studies were performed using confocal microscopy. We observed a strong and clear co-localization with ER markers, but not with the Golgi with both constructs (Fig 2B for N-terminal tag and Suppl Fig 1A for C-terminal tag). ER co-localization was also observed in TAP-negative cells (Suppl Fig 1B). An intermediate degree of co-localization with mitochondria was found (Fig. 2B). It is known that the CerS1, CerS2 and CerS6 ceramide synthases can indeed be detected in mitochondria[33], but, alternatively, this mitochondria co-localization might merely reflect ER membranes that are in close proximity of mitochondria. These data indicate that Trh4 is a multimembrane spanning protein in ER membranes and that its C-terminal tail, comprising the epitope, docks into this membrane directing towards the ER lumen.

Inhibitors of intramembranous aspartyl proteases prevent peptide liberation

Next, we investigated which family of proteases was responsible for the proteolytic cleavage of Trh4 resulting in liberation of the C-terminal peptide. An array of inhibitors blocking hydrolysis by different classes of proteases were applied in a recovery assay in which TAP-deficient RMA-S cells were briefly acid stripped to remove cell surface MHC-I and allow for re-emergence of Trh4/D^b peptide complexes. Complete recovery of Trh4/D^b was reached within six hours, as determined with a peptide-specific T cell clone (Fig 3A). This highlighted a continuous and efficient supply of Trh4 peptide from this alternative processing pathway. Two enzymes were likely candidates, since they were described to result in TAP-independent peptide loading: signal peptidase and furin[20, 21]. However, the specific inhibitors DCI and Dec-RVKR-CMK, respectively, failed to impair the generation of Trh4/D^b complexes (Fig 3B), indicating that Trh4 processing is mediated by a novel mechanism. In line with our previous data, inhibition of the proteasome rather

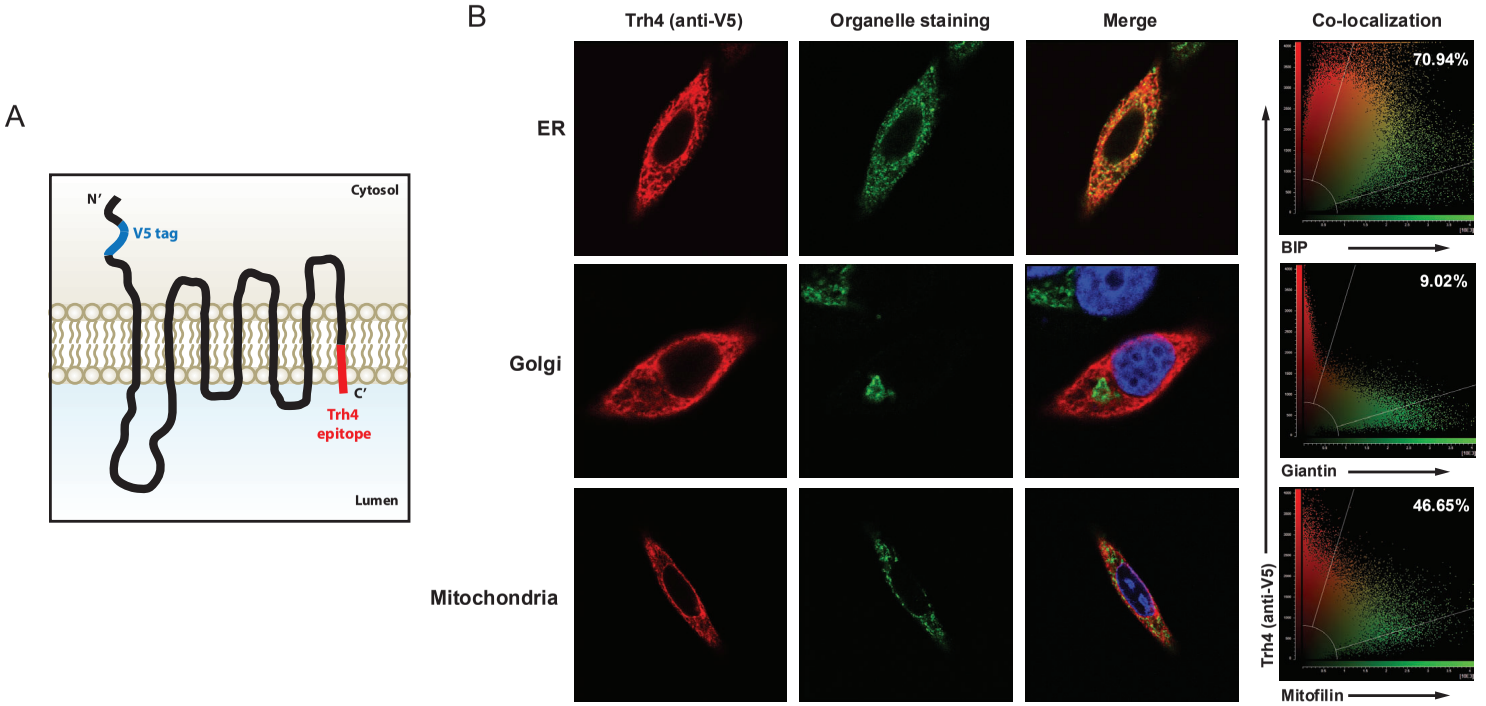

Figure 2. The C-terminal tail of Trh4 is localized within the ER membrane. (A) Prediction of the Trh4 topology in membranes according to algorithm software (www.predictprotein.org). The C-terminal peptide-epitope is indicated in red. (B) Confocal microscopy imaging of V5-tag at the N-terminus of Trh4 protein in combination with staining for endoplasmic reticulum (BIP), Golgi (giantin) or mitochondria (mitofilin). Mean percentages of colocalization were calculated on ten images of at least three independent experiments.

increased Trh4/D^b complexes (Fig 3B), suggesting that the proteasome somehow acts as a competitor for the novel processing mechanism[28].

Next, we observed that the common calpain inhibitor calpeptin partly decreased Trh4 presentation at relatively high concentrations (> 20 uM) (Fig 3C and Suppl Fig 2A). The main targets for calpeptin are calpain 1 and calpain 2. We determined the expression of these two calpain members in RMA-S cells and observed that calpain 2 was expressed but calpain 1 was not detectable (Suppl Fig 2B). Therefore, we silenced the expression of calpain 2, but this did not lead to reduced Trh4/D^b peptide complexes at the cell surface

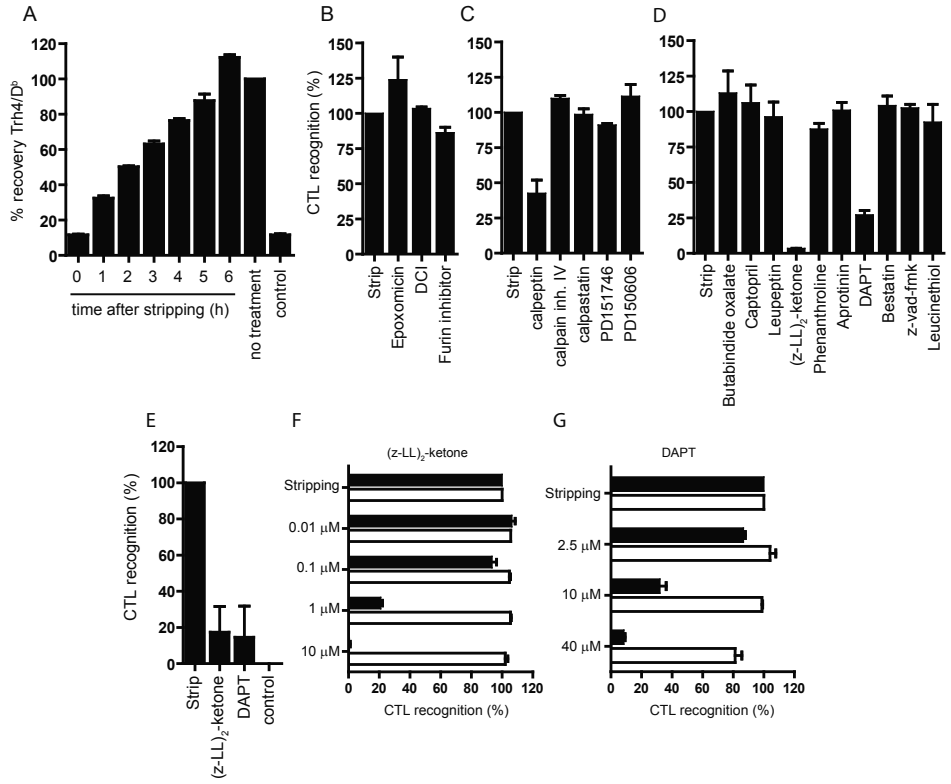

Figure 3. The D^b-presentation of the Trh4-derived peptide is generated by intramembrane-cleaving aspartyl proteases. (A) Recovery kinetics of Trh4/D^b complexes on TAP-deficient RMA-S cells after brief stripping with mild acid buffer. Cells were tested with Trh4-specific T cell clone in intracellular IFN-γ staining. (B) Recovery efficiency of Trh4/D^b complexes was tested in the presence of an array of protease inhibitors. Inhibitors of proteasome and enzymes known to be involved in TAP-independent processing pathways, (C) inhibitors of calpain family, (D) all other tested inhibitors. (E) TAP-deficient fibrosarcoma MCA cells were tested with inhibitors for aspartyl proteases. (F) Concentration range of the functional inhibitor (z-LL)$_2$-ketone and (G) DAPT on RMA-S cells. Trh4-specific T cells (filled bars) were used and control T cells (open bars) that recognize an independent K^b-presented peptide on RMA-S. All panels show compiled means and standard deviations from at least three independent experiments, setting the recovered cells at 100%.

(Suppl Fig 2C-D). Furthermore, more selective inhibitors for the calpain family did not affect the CTL response, collectively suggesting that the marginal blocking effect by calpeptin was based on cross-reactivity to other proteases (Fig 3C).

We then continued the screen with several other classes of chemical inhibitors targeting serine-, cysteine-, aspartyl- and metallo-proteases, and aminopeptidases (Fig 3D). The results revealed two inhibitors for aspartyl proteases, $(z\text{-}LL)_2$-ketone and DAPT, that strongly decreased presentation of the Trh4-derived peptide. Importantly, none of the other eight protease inhibitors influenced the Trh4/D^b presentation, suggesting that the involved aspartyl protease was necessary and sufficient. The inhibitory effect was also observed when we tested fibrosarcoma cells, indicating that the inhibition was not cell-type restricted (Fig 3E). Titration of the two active compounds demonstrated a 50% decrease at concentrations in the lower range in this cellular assay, 300 nM for $(z\text{-}LL)_2$-ketone and 5 uM for DAPT (Fig 3F and G). These concentrations were clearly not toxic for the target cells and, moreover, recognition of treated RMA-S cells by control T cell clones specific for another peptide epitope was unaltered, excluding a general defect in the MHC class-I presentation capacity by $(z\text{-}LL)_2$-ketone and DAPT (Fig 3F and G). These two compounds were known to target aspartic acid proteases that are located within membranes, particularly members of the signal peptide peptidase (SPP) family[34, 35]. Interestingly, calpain inhibitors were shown to block the action of SPP at higher concentrations, corroborating our findings in the screen with calpeptin (Fig 3C)[36]. Together, these results let us conclude that the liberation of the C-terminal Trh4 peptide within the ER membrane is part of a novel processing pathway for TAP-independent peptides and is distinct from the previously described routes.

Signal Peptide Peptidase is responsible for the processing of the C-terminal peptide

The SPP family is also known as intramembrane-cleaving proteases (I-CLiPs) of the aspartyl type and this family is involved in many biological processes, including cell proliferation, differentiation and immunity[34, 37, 38]. SPP and SPPL3 were reported to be localized in ER membranes, forming catalytic cavities in which hydrolysis can take place within membranes[39]. We first analyzed the expression of the family members at mRNA level in the tumor cell lines active in Trh4 peptide processing (Fig 4A). All family members were expressed to varying degree in this cell panel, except SPPL2c, which was hardly detectable. High levels of SPP were measured in all cells. Differences in expression levels in the tumor cell panel prompted us to profile transcripts of these genes in normal mouse tissues, especially since this information is lacking in the current literature (Suppl Fig 2E). RNA extracts from whole mouse organs were analyzed for these intramembrane aspartic peptidases and a general low expression for SPPL2b and SPPL2c was found. Similar expression profiles were seen for SPP, SPPL2a and SPPL3 in that thymus and brain contained low transcript numbers and lung was high (Suppl Fig 2E).

Next, we wanted to determine which family member was responsible for the liberation of the C-terminal Trh4 peptide in tumor cells and silenced each gene individually using

short hairpin RNA constructs. SPPL2c was not included in this analysis, since it was not expressed in the tumor cells (Fig 4A). Efficiency of gene silencing was approximately 50-60% for all genes and, importantly, the shRNA constructs were specific in that the other members were not targeted (Fig 4B). We then used this cell panel to determined effects on recognition by Trh4-specific CTL. Downregulation of SPP clearly decreased the recognition by these CTL (Fig 4C). Similar decrease of Trh4 peptide presentation was observed in TAP-negative MCA fibrosarcoma cells (Suppl Fig 2F-G). Silencing of the other SPP family members resulted in a marginal variation of CTL recognition (Fig 4C). The presentation of the Trh4 peptide was not completely blocked by SPP silencing, most likely due to a substantial residual expression of the protease. The residual CTL recognition could furthermore be blocked by $(z\text{-}LL)_2$-ketone, supporting this notion. Importantly, an independent other peptide-epitope presented by RMA-S was not affected by SPP silencing (Fig 4D). These data and the fact that SPP is expressed in all mouse cells that naturally display Trh4/D^b complexes and the ER localization of Trh4 substantiate the conclusion that the SPP enzyme is crucial for the processing of the C-terminal peptide-epitope of Trh4 in a TAP-independent way.

The transmembrane region directly upstream of the Trh4 peptide is crucial for Trh4 processing

To study the underlying mechanism of Trh4 peptide processing in detail and to determine critical regions for the proteolytic process, extensive mutagenesis analysis of Trh4 was performed. First, some larger segments at the N- and C-terminus of the protein were deleted. Removal of the first 32 aa did not diminish the processing efficiency of the peptide-epitope (Fig 5A), whereas we hypothesized that this region functioned as a leader sequence routing the protein to the ER, as indeed was predicted by the online SignalP 4.1 Server (www.cbs.dtu.dk). Confocal microscopy analysis however confirmed that this construct was still localized in ER (Suppl Fig 1C). We then removed segments located near the C-terminus, starting with the sequence corresponding to amino-acids 340-374, which is a cytosolic loop located between the two last transmembrane domains (see Fig 2A). We did a progressive deletion in this construct comprising the upstream amino-acids 315-330, which includes most of the second last transmembrane domain. However, none of these large deletions decreased Trh4 peptide processing (Fig 5A). In order to exclude the possibility that these altered constructs delivered defective and thus proteasome-targeted proteins, we confirmed that the Trh4 peptide presentation from these mutant constructs was still $(z\text{-}LL)_2$-ketone and DAPT dependent (Fig 5B). Then, nine amino-acids just upstream of the C-terminal peptide were removed. This resulted in a more than 60% impairment of CTL recognition (Fig 5A), indicating that this intramembrane stretch, just upstream of the peptide-epitope was critical for SPP cleavage. Furthermore, the C-terminus was extended by cloning small V5-containing tags of 14 and 47 amino-acids. Although these proteins were properly expressed, as tested by western blot (Suppl Fig 3A), and were localized in the ER (Suppl Fig 1A), they did not result in any Trh4 peptide presentation (Fig 5A), implying

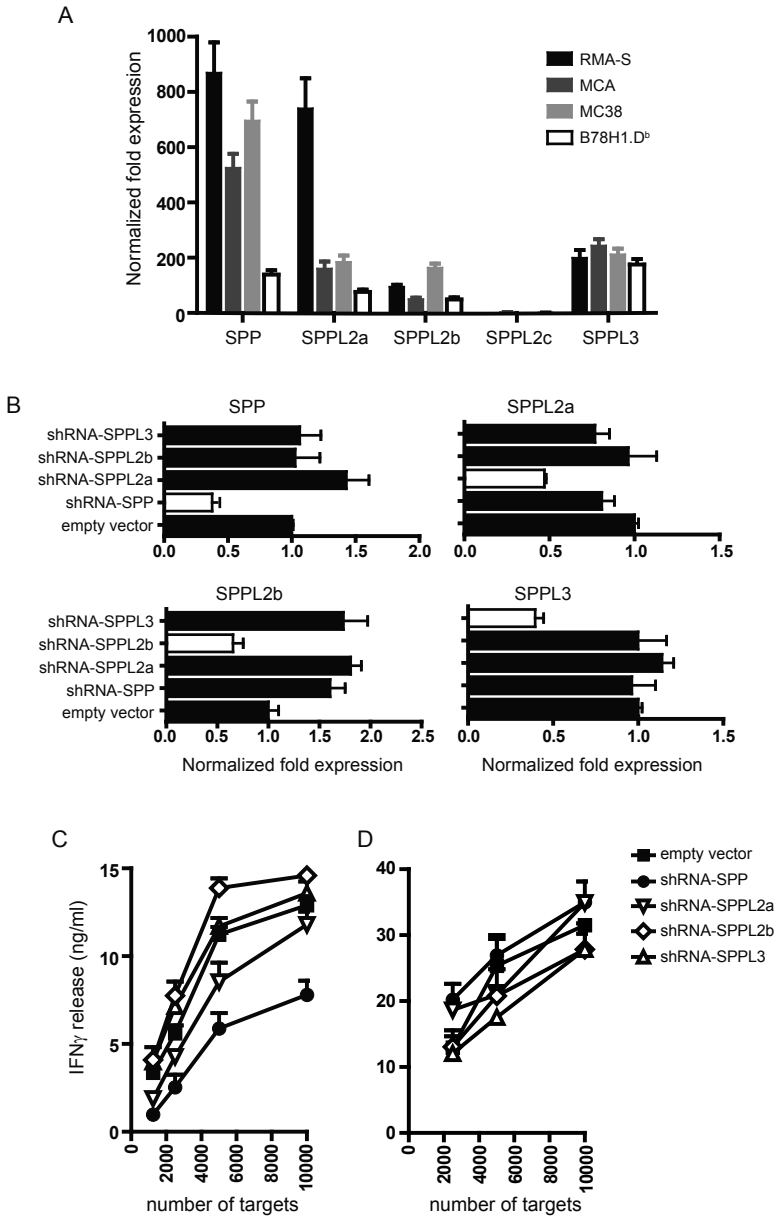

Figure 4. The intramembrane-cleaving signal peptide peptidase is involved in Trh4 processing. (A) mRNA expression of *SPP*, *SPPL2a*, *SPPL2b*, *SPPL2c* and *SPPL3* genes was determined by qPCR in tumor cell panel. (B) Silencing of SPP family members in RMA-S cells was reached by lentiviral transfer of shRNA constructs. Empty shRNA vector served as control. Efficiency and specificity of downregulated levels is shown as measured by qPCR. (C-D) Cell panel with silenced single SPP family members was tested for recognition by Trh4-specific T cells (C) or control T cells (D) reactive to the independent K^b-presented peptide mi3 by RMA-S. Mean and standard deviation from one out of three experiments is shown. Difference between SPP and control vector is statistically significant ($p<0.001$, two way Anova test). Similar data were obtained in the fibrosarcoma cell line (Suppl Fig 2F-G).

that the C-terminal location of the peptide in the Trh4 protein is crucial for its liberation. Failure to process the Trh4 peptide when it was not at the complete C-terminus might be related to the absence of carboxyl-peptidases in the ER and suggests that the SPP cleavage products do not travel through the cytosol. Furthermore, we also tested if the C-terminal region would function as a leader sequence for the Trh4 protein, but removal of the last 20 amino-acids (aa368-387) did not change its subcellular localization (Supp Fig 1D). We therefore concluded that Trh4 peptide is directly liberated by SPP from the mature protein after which the peptide is available in ER for loading into MHC-I molecules.

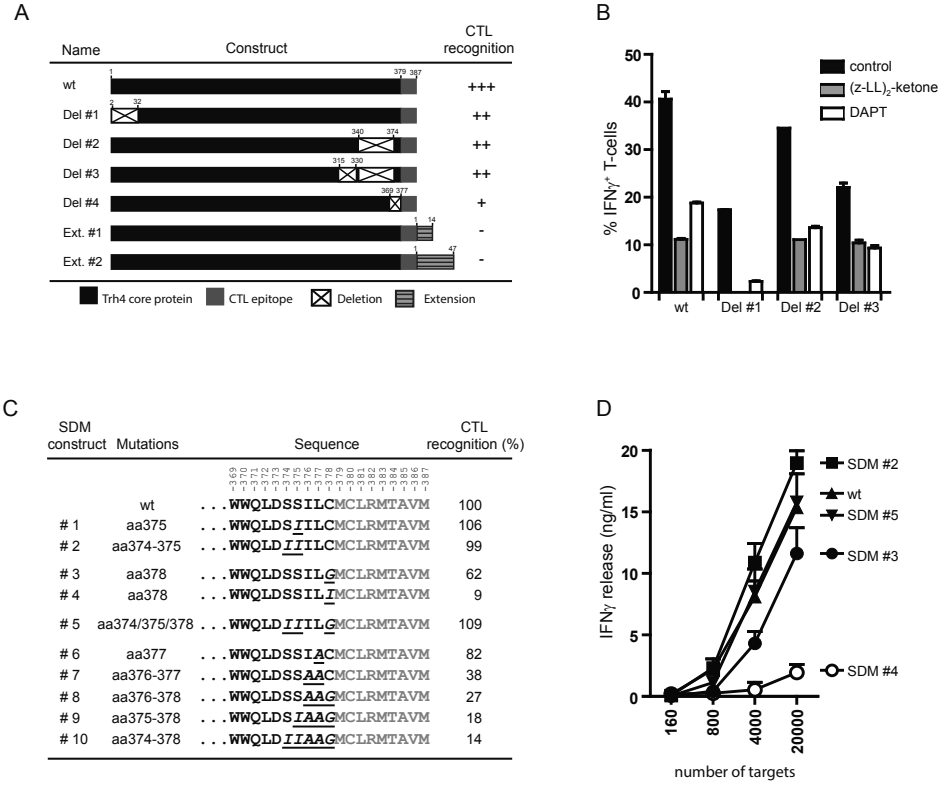

Figure 5. The intramembrane region directly upstream of the Trh4 peptide is crucial for processing. (A-B) Trh4 constructs with deletions or extensions were tested for liberation and MHC-I presentation of the C-terminal peptide-epitope (aa379-387). (A) DNA plasmid constructs were transiently transfected into HeLa cells together with the mouse D^b gene. Extend of IFN-γ release by T cells was quantified and scored as "+++" (wild-type construct, 100%), "++" (50-90%), "+" (10-50%) and "-" (<10%). (B) Processing from mutant constructs was still sensitive for the protease inhibitors $(z\text{-}LL)_2$-ketone and DAPT. All constructs were tested at least four times. (C-D) Site-directed mutagenesis directly upstream of the C-terminal peptide-epitope of the Trh4 gene. (C) The amino-acid substitutions and the position of the amino-acids in the protein are indicated. Degree of T cell recognition was quantified based on 'area under the curve' values of line graphs as shown in (D). Compiled means and standard deviations of at least three independent experiments is shown in Suppl Fig 3B.

The importance of the direct upstream amino-acids of the Trh4 peptide suggested that the SPP cleavage site was located within this last membrane region (aa374-387). Single amino acid substitutions were introduced using site-directed mutagenesis to determine the precise requirements for cleavage by SPP. Several publications demonstrated the strong preference of SPP for substrates with helix-destabilizing residues in their transmembrane domain[40-42]. Amino-acids like asparagine, serine and cysteine disturb a perfect alpha-helical conformation of the transmembrane domain and are therefore referred to as 'helix-bending' or 'helix-breaking' residues. Three of such amino-acids are present in the Trh4 membrane region: two serines (aa374 and 375) and one cysteine (aa378) (Fig 5C). First, the two serines were replaced by isoleucines, which strongly contribute to a perfect alpha-helical structure. In contrast to our expectations, these mutations did not affect Trh4 presentation at all (Fig 5C and D; SDM #2). Second, the cysteine residue (aa378) in front of the epitope was substituted for a glycine (SDM #3), which still has some helix-breaking capacity, or an isoleucine (SDM #4), which removes the helix-breaking nature. These alterations had a very strong impact on peptide liberation and the C378I construct nearly completely failed to produce the Trh4 peptide. Third, we combined the cysteine mutation C378G with the serine mutations and surprisingly found that introduction of two isoleucines improved the Trh4 processing (Fig 5C and D; SDM #5), indicating that the more upstream serine residues were actually counterproductive for optimal SPP cleavage and support the importance of the cysteine residue directly upstream of the epitope. Fourth, we progressively substituted the complete stretch of amino-acids in this region also using alanines which are considered to promote helix-destabilization[43]. Collectively, these constructs displayed a clear gradual decrease in peptide presentation (Fig 5C and Suppl Fig 3B). Together, these data point to the importance of the cysteine directly upfront of the epitope, most likely marking the actual SPP cleavage site and suggest that nearby flanking residues indirectly influence this process via conformational change in the intramembrane alpha-helix. In line with this hypothesis is the finding that presentation of the Trh4 peptide does not depend on the N-terminal trimming peptidase ERAAP (Fig 3D), suggesting that the minimal 9-mer epitope is directly generated by SPP cleavage without further need for C-terminal nor N-terminal trimming. The C-terminal liberation of this CTL peptide-epitope by the aspartyl protease SPP within the ER membrane exemplifies a novel way by which TAP-deficient cells are still able to present a diverse antigen repertoire.

Contribution of SPP protease family to MHC-I peptide repertoire of TAP-negative cells

We further examined the contribution of the SPP family of proteases to the overall MHC-I presentation of TAP-deficient cells. We analyzed the surface display of the two alleles of this mouse strain, D^b and K^b, on RMA-S cells in which individual SPP members were silenced by shRNAs. SPP and SPPL2a silencing resulted in reduction of K^b molecules to 77% and 65% of control, respectively (Fig 6). The presentation of D^b molecules on these cells and MHC-I surface display on RMA-S cells in which SPPL2b

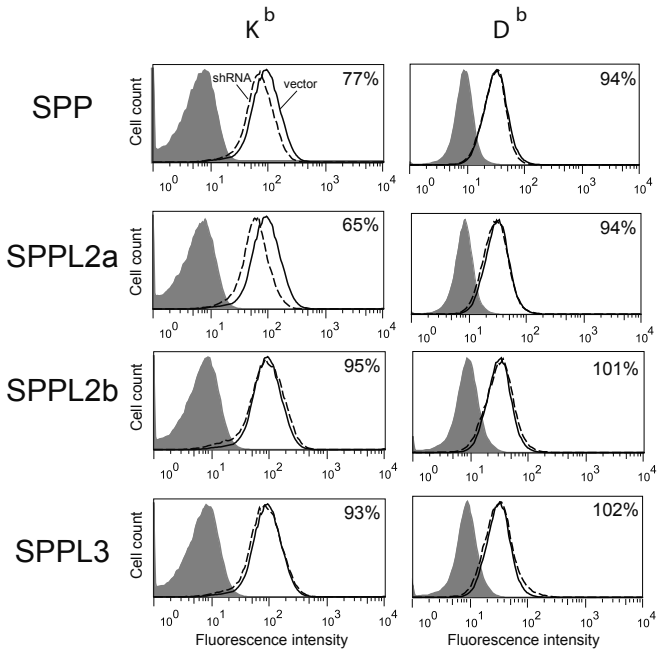

Figure 6. Silencing of SPP and SPPL2a leads to decrease in surface MHC-I. MHC-I surface display of RMA-S cells expressing shRNA constructs for SPP, SPPL2a, SPPL2b and SPPL3 was measured by flow cytometry (K^b and D^b molecules separately). Percentages in the upper right corners reflect the residual MHC-I expression compared to control cells ('vector'), based on mean fluorescence intensity. Data are representative for three independent experiments.

and SPPL3 were silenced, was not affected (Fig 6). These data underline the involvement of intra-membrane cleaving proteases in antigen processing, although precise underlying mechanisms remain to be elucidated.

| DISCUSSION

Studies with TAP-deficient cells showed that peptides can still gain access to MHC-I molecules, although with much lower efficiency. This peptide repertoire is different from that of processing-intact cells, indicating that alternative processing pathways partly compensate for a defective conventional route based on proteasome and TAP[14, 18, 19]. The processing mechanisms that lead to presentation of TAP-independent peptides are poorly characterized. Here we describe a new mechanism that leads to liberation of a C-terminal peptide-epitope from the ER membrane-spanning Trh4 protein. We found that the intramembrane-cleaving enzyme SPP was responsible for the cleavage event at the direct upstream region of the T cell epitope within the lipid bilayer. We speculate that SPP activity in the ER membrane is sufficient to liberate the minimal 9-mer peptide and release of this peptide into the ER lumen. Additional N-terminal trimming of the

cleavage product is unlikely, since inhibitors of amino-peptidases did not prevent Trh4 peptide presentation and the cysteine just upfront of the 9-mer epitope appeared to be critical in the SPP cleavage process (see Fig 3 and 5C). Moreover, direct release of the liberated peptide into the ER lumen is very likely, due to the type II transmembrane orientation of the Trh4 protein tail (see Fig 2A) and the fact that the epitope is located at the very C-terminal end of the protein. The incompetence of C-terminally extended versions of Trh4 to present the peptide (see Fig 5A) corroborate the idea that the peptide is directly released in the ER lumen where it needs a free C-terminus for loading into MHC-I molecules. The exact peptide loading mechanism of the Trh4 membrane peptide however remains to be determined.

The involvement of SPP in the C-terminal processing of a transmembrane protein initially surprised us. The activity of SPP was thus far largely related to the removal of small trunks of signal-sequence-derived transmembrane peptides from the ER membrane[34, 37, 42]. The processing of leaders from nascent proteins requires a first cut by signal peptidase (SP), after which the remaining transmembrane stretch is cut in two parts by SPP. However, the liberation of the Trh4 peptide did not require SP activity, since its inhibitor DCI did not prevent the presentation of the epitope. Furthermore, the Trh4-peptide is not part of a signal sequence and removal of the N- or C-terminal domain did not route the Trh4 protein to a different subcellular localization (see Suppl Fig 1C-D). Nevertheless, the involvement of SPP with Trh4 cleavage fits with the strong preference for type II membrane segments and with the 'helix-breaking' residues that are often found in SPP target proteins[25, 41, 42]. Therefore it seems that the role of SPP is more extended than the release of transmembrane leader-sequences form the ER membrane. Interestingly, it has been suggested that SPP is physically associated with misfolded membrane proteins[44, 45] and as such might function as a chaperone to dispose membrane aggregates.

The Trh4-derived peptide is an example of TAP-independently processed peptides. This particular SPP-mediated processing pathway is operational in TAP-negative as well as TAP-positive cells (see Fig 1) and also in tumor as well as healthy cells[28]. Therefore, the TAP-independent pathway described here seems to be part of the "normal activity" of cells and does not represent a disease-related feature. Over the years, some other TAP-independent pathways have been characterized. They comprise peptides generated in the secretory and vesicular compartments by the protein convertase furin[22, 23]. Second, leader sequence derived peptides are frequently TAP-independently processed[24]. Peptides that arrive in the ER via this way overcome the need of TAP transport. Interestingly, TAP-independent processing was observed earlier using several C-terminally tagged constructs of ER-targeted proteins, feeding the speculation on a common 'C-terminal' processing rule[46, 47]. We hypothesize that SPP might be a central player for this category of TAP-independent antigen processing.

The family of intramembrane-cleaving aspartyl proteases (SPP family and presenilins) have important biological roles in signal transduction, cell differentiation and immunity[25, 48]. For instance, SPPL2a and SPPL2b were shown to be responsible for the release of the

TNF-α intracellular domain, leading to expression of the pro-inflammatory cytokine IL-12 in dendritic cells[38] and also for the release of the intracellular domain of fasL in T cells[49]. These proteases are mainly located in the vesicular pathway and at the cell surface. Recently, SPPL2a was reported to be involved in the proteolysis of the invariant chain (CD74) and thereby critical for the development and survival of B-cells and DCs[50-52], maybe explaining the effect we found on MHC class I expression (Fig 6). We now extend on the involvement of SPP family members in immunity by showing their role in alternative pathways of MHC-I antigen processing, thereby enabling T cell immune responses.

| MATERIAL AND METHODS

Cell lines

The mouse tumor cell lines RMA, RMA-S (TAP2-deficient), MCA (TAP1-deficient), MC38, B78H1 (TAP2-deficient) and human HeLa and 293T have been described previously[14, 17, 28]. Where indicated, cell lines were transfected with H-2D^b or Trh4 genes (accession numbers: gene BC043059 (www.ncbi.nlm.nih.gov/nuccore), protein UniProtKB Q9D6K9-2 (www.uniprot.org/uniprot) via retroviral transduction using the LZRS vector containing GFP behind an internal ribosome entry site[16]. The mouse TAP genes were introduced into MCA and B78H1 cells by gene transfer. MC38.UL49.5 cells contain the UL49.5 gene from the Bovine Herpes Virus-1 which blocks mouse TAP activity[16, 29].

Generation and culture of CD8$^+$ T cell clones used in this study were previously described: D^b-restricted CTL clone B5 specific for the TAP-independent Trh4 peptide (MCLRMTAVM); K^b-restricted CTL clone mi3 specific for a yet unknown TEIPP peptide and the D^b-restricted CTL clone 1 specific for the TAP-dependent MuLV gag-leader peptide (CCLCLTVFL)[16, 17, 30].

All cells were cultured in complete IMDM medium (Invitrogen, Carlsbad, CA) containing 8% heat-inactivated FCS, 100 U/ml penicillin, 100 μg/ml streptomycin (Life Technologies, Rockville, MD), 2mM L-glutamine (Invitrogen) and 30 μmol/L of 2-mercaptoethanol (Merck, NJ, USA) at 37°C in humidified air with 5% CO2.

Protease inhibitor experiments

Cells were resuspended in X-vivo medium (Lonza) supplemented with 0,5% of BSA and incubated with protease inhibitors for 1h at 37°C, under continuous mixing. Cells were incubated for 2-4 min with mild acid citrate/phosphate buffer (pH 3.1) at room temperature to disrupt MHC class I/peptide complexes[28]. Cells were washed twice and incubated with protease inhibitors for additional 6h under the conditions mentioned above and then treated with brefeldin A. Inhibitor-treated cells were then incubated with the indicated T cell clones for 18h in the presence of brefeldin A and intracellular stained for IFNγ production[28]. Chemical inhibitors used in these assays are: epoxomicin (1μM, Sigma-aldrich), 3,4-Dichloroisocoumarin (5μM, Sigma-aldrich), Decanoyl-RVKR-CMK (10μM, Merck), calpeptin (30μM, Merck), calpain inhibitor IV (13μM, Merck), calpastatin

peptide (10μM, Merck), PD151746 (50μM, Santa Cruz Biothecnology), PD150606 (50μM, Santa Cruz Biothecnology), butabindide oxalate (400μM, TOCRIS Bioscience), captopril (100μM, Sigma-aldrich), leupeptin (100μM, Merck), $(z\text{-}LL)_2$-ketone (5μM, Merck), 1,10-Phenanthroline monohydrate (400μM, Sigma-aldrich), aprotinin (10μM, Merck), DAPT (10μM, Sigma-aldrich), Bestatin hydrochloride (100μM, Sigma-aldrich), z-vad-fmk (10μM, Merck), L-leucinethiol (60μM, Sigma-aldrich) and DL-Dithiothreitol (5mM, Sigma-aldrich). None of the inhibitors was toxic at the applied concentrations, as determined by trypan-blue counting and annexin-V staining.

T-cell activation assays and flow cytometry

Intracellular cytokine staining of IFN-γ in T cell clones was performed for the protease inhibitor screen and expressed as percentage positive cells[31]. IFN-γ secretion by T-cell clones was measured by ELISA as previously published[28]. Data shown represent mean values obtained from triplicate test wells and error bars represent standard deviation of these values. Flow cytometry analysis of surface expression of D^b and K^b molecules was performed using directly labeled anti-D^b mAb (clone 28.14.8S; BioLegend, California, USA) and anti-K^b mAb (clone AF6-88.5, BioLegend). Cells were measured using a FACS Calibur and analysed with Flowjo software (Tree Star, Ashland, OR).

Quantitative PCR analysis

Total RNA isolation was performed using RNeasy Mini Kit (Qiagen, Maryland, USA). 500 ng of purified total RNA was used to synthesize cDNA using High Capacity RNA-to-cDNA Kit (Applied Biosystems, Foster City, USA). Quantitative PCR on two different transcripts of Trh4 was done using unique forward primers. Forward primer for the Trh4-epitope containing transcript 5'-GCAGACCCCTTACTGGAAGCTGC-3' and for the short transcript 5'-TACATCACTGCGGTCATC-3'. Common reverse primer was 5'-CTGCGGTCATCCTTAGACACCTTTCC-3'. The primers used to detect the expression of mouse transcripts from SPP, SPPLs and calpains were designed by us using the Beacon designer software and are listed in Supplementary Table 1 (calpain family) and Table 1 (SPP family). All primer sets were validated to be specific for the cognate genes by sequencing of the amplified PCR products. For the PCR reaction SensiMix™ SYBR No-ROX kit from GC Biotech Bioline (Alphen aan den Rijn, Netherlands) was used in a C1000™ Thermal Cycler (Bio-Rad, Hercules, CA, USA) and results were analysed using Bio-Rad CFX manager software.

Table I. Primer sequences for quantitative PCR for the mouse SPP family.

Name	Gene ID	Forward primer (5'->3')	Reverse primer (5'->3')	Size (bp)
SPP	14950	CAGGATCTGCTGGAGAAG	GAAGTAGGTGTGCGTGTT	138
SPPL2a	66552	CTGATGGCATAAGGAACAAG	GAGGAAGGAATTAGGACACT	133
SPPL2b	73218	CATTGCCTTCTGCCTGTA	GATGCTGTTGCCACTCTT	142
SPPL2c	237958	TGCATTGCCTCTGCTGTGGGC	TGTGGCCCTCTGGACTCGTGG	181
SPPL3	74585	TCGCTATGACAACTACAAGA	GCAGTGGAAGTAGGAGAC	93

Confocal microscopy

Human HeLa cells or mouse MCA cells were plated in 12-wells plates on glass coverslips and transfected the next day with the indicated Trh4 gene constructs using Lipofectamine 2000 (Invitrogen) according to the manufacturer's protocol. After one day cells were stained with monoclonal antibodies: cells were fixed with methanol for 30 minutes at 4˚C, washed with TBSB (TBS with blocking reagent from Boehringer Mannheim) and incubated for 1.5 hours at room temperature with the first antibody diluted in 500 µl TBSB. The antibodies used were anti-V5 (Invitrogen, R960-25), anti-Giantin (Abcam, ab24586) and anti-BIP (Abcam, ab21685). Cells were then washed again with TBSB and incubated with second antibodies; anti-rabbit-Alexa488 (Invitrogen, a11008) and anti-mouse-Alexa594 (Invitrogen, a11005) for 1.5 hours at room temperature. Finally, cells were washed with TBSB and the coverslips were put on microscope glass slides with 5µl of ProLong Gold antifade reagent (Invitrogen) containing Hoechst (Enzo, Hoechst 33342). The stained cells were imaged with a TCS SP5 fluorescent confocal microscope (Leica, Germany) using LAS AF software. Stained samples were observed at room temperature. All images were acquired with a 63X glycerol immersion objective lens NA 1.4 (Leica). Analysis of colocalization was performed with LAS AF software (Leica).

shRNA treatment

MISSION® shRNA constructs specific for mouse SPP, SPPL2a, SPPL2b, SPPL3 and calpain 2 were obtained from Sigma-Aldrich and lentiviral encapsulation was reached in HEK.293T cells via transfections with calcium phosphate (Promega) of pCMV-VSVG, pMDLg-pRRE, pRSV-REV and pLKO plasmid with puromycin resistance gene and a shRNA sequence or empty vector. RMA-S cells were incubated with lentivirus particles encoding shRNA and particles encoding GFP in a 10:1 ratio for 20h at 37°C. Then the cells were washed and resuspended in complete medium supplemented with 1µg/ml of puromycin and cultured for 4 days. GFP expressing cells were sorted and used in experiments.

Trh4 gene constructs

Length variants of Trh4 (deletions and extensions) were performed on the cloned cDNA (accession number BC043059) in pcDNA3.1 plasmid. C-terminal extensions were created by removing the stop codon of Trh4 in the pcDNA3.1/V5-His vector (Invitrogen, Life Technologies), resulting in the in frame encoding V5 antibody epitope. The deletion variants were based on an N-terminally tagged V5 construct in which the antibody site was introduced after nucleotide nr 96, which was supposed to be the leader sequence. We introduced a NOT-I restriction site at this place by creating two complementary PCR products, resulting in two altered amino acids at position 32-33 (from DL to AA). Then the 14 aa long V5 sequence was introduced at this NOT-I site using long synthetic oligonucleotides including NOT-I overhangs. Orientation and sequence of this insert was validated by sequencing. This 'N-terminal' tagged Trh4 construct was then used to create several deletion variants using PCR primer sets. All PCR amplifications were performed with Accuprime kit (Invitrogen).

Site-directed mutagenesis was done on the N-terminal V5 construct in pcDNA3.1 using USB Change-IT Multiple Mutation Site Directed Mutagenesis technology (Affymetrix). Generated clones were sequenced to validate the introduced changes.

Western blot

Cells were lysed in 1% Nonidet P-40 lysis buffer (50 mM Tris-HCl, 150 mM NaCl (pH 8.0), 1% NP40, 1mM leupeptin, 1mM 4-(2-aminoethyl)-benzene-sulfonyl fluoride hydrochloride (Sigma-Aldrich,The Netherlands). The samples were mixed 1:1 with sample buffer (0,1 M Tris (pH 8.0), 4% SDS, 20% glycerol, 10% 2-mercaptoethanol, 0.05 % bromophenolblue) and heat up to 95°C for 1 minute. The samples were loaded in pre-cast gels 4-15% (BioRad) using the Mini-PROTEAN® Tetra 4-gel vertical electrophoresis system (BioRad). The BenchMark Pre-Stained Protein Ladder (Invitrogen) was included. Gels ran for 25 min at 250V and blotted in Trans-Blot® Turbo™ Transfer System (BioRad) according to the manufacturer recommendations. After blotting, the membrane was incubated overnight at 4°C in 5% low-fat milk/TBST (10 mM Tris-base, 150 mM NaCl, 0.05% Tween 20, pH 7.4). The next day the blots were stained with anti-V5 monoclonal antibody 1:2500 (Invitrogen) in 1% low-fat milk/TBST for 2 hours at room temperature. After the staining, the membrane was washed three times for 5 min in TBST. Next, the membrane was incubated with HRP-labeled goat anti-mouse Ig antibody (1:2000) in 1% low-fat milk/TBST for 2 hours at room temperature, followed by three times washing in TBST and three times in TBS. Visualization of the blot was performed using ECL Plus Western blotting detection reagents (GE Healthcare) on films.

| ACKNOWLEDGEMENTS

We like to acknowledge Dr Pieter van der Pol, Nicole Schlagwein and Joop Wiegant (LUMC, Netherlands) for their help in immunofluorescent confocal microscopy. Dr. Isaac Donkor (Memphis, Tennessee, USA) kindly provided specific calpain inhibitors and Dr Ramon Arens is acknowledged for critical reading of the manuscript.

Financial support was received from Portuguese Foundation For Science and Technology (MCTES) Portugal (SFRH/BD/33539/2008 to CCO).

| REFERENCES

1. Cresswell, P., Ackerman, A.L., Giodini, A., Peaper, D.R. & Wearsch, P.A. Mechanisms of MHC class I-restricted antigen processing and cross-presentation. *Immunol. Rev.* **207**, 145-157 (2005).
2. Rock, K.L., Farfan-Arribas, D.J. & Shen, L. Proteases in MHC class I presentation and cross-presentation. *J Immunol* **184**, 9-15 (2010).
3. Vyas, J.M., Van der Veen, A.G. & Ploegh, H.L. The known unknowns of antigen processing and presentation. *Nat Rev Immunol* **8**, 607-18 (2008).
4. Kessler, J.H. et al. Antigen processing by nardilysin and thimet oligopeptidase generates cytotoxic T cell epitopes. *Nat Immunol* **12**, 45-53 (2011).
5. Seifert, U. et al. An essential role for tripeptidyl peptidase in the generation of an MHC class I epitope. *Nat Immunol* **4**, 375-9 (2003).
6. Aldrich, C.J. et al. Positive selection of self- and alloreactive CD8+ T cells in TAP-1 mutant mice. *Proc. Natl. Acad. Sci. USA* **91**, 6525-6528 (1994).

7. Sandberg, J.K., Chambers, B.J., Van Kaer, L., Karre, K. & Ljunggren, H.G. TAP1-deficient mice select a CD8+ T cell repertoire that displays both diversity and peptide specificity. *Eur. J. Immunol.* **26**, 288-293 (1996).
8. Van Kaer, L., Ashton-Rickardt, P.G., Ploegh, H.L. & Tonegawa, S. TAP1 mutant mice are deficient in antigen presentation, surface class I molecules, and CD4-8+ T cells. *Cell* **71**, 1205-14 (1992).
9. Cerundolo, V. & de la Salle, H. Description of HLA class I- and CD8-deficient patients: Insights into the function of cytotoxic T lymphocytes and NK cells in host defense. *Semin Immunol* **18**, 330-6 (2006).
10. Zimmer, J. et al. Clinical and immunological aspects of HLA class I deficiency. *QJM* **98**, 719-27 (2005).
11. de la Salle, H. et al. Human peptide transporter deficiency: importance of HLA-B in the presentation of TAP-independent EBV antigens. *J Immunol* **158**, 4555-63 (1997).
12. Lautscham, G. et al. Identification of a TAP-independent, immunoproteasome-dependent CD8+ T-cell epitope in Epstein-Barr virus latent membrane protein 2. *J Virol* **77**, 2757-61 (2003).
13. Chambers, B. et al. Induction of protective CTL immunity against peptide transporter TAP-deficient tumors through dendritic cell vaccination. *Cancer Res* **67**, 8450-5 (2007).
14. Oliveira, C.C. et al. The nonpolymorphic MHC Qa-1b mediates CD8+ T cell surveillance of antigen-processing defects. *J Exp Med* **207**, 207-21 (2010).
15. Seidel, U.J., Oliveira, C.C., Lampen, M.H. & Hall, T. A novel category of antigens enabling CTL immunity to tumor escape variants: Cinderella antigens. *Cancer Immunol Immunother* **61**, 119-25 (2012).
16. Van Hall, T. et al. The varicellovirus-encoded TAP inhibitor UL49.5 regulates the presentation of CTL epitopes by Qa-1b. *J Immunol* **178**, 657-62 (2007).
17. Van Hall, T. et al. Selective cytotoxic T-lymphocyte targeting of tumor immune escape variants. *Nat. Medicine* **12**, 417-424 (2006).
18. Lampen, M.H. et al. Alternative peptide repertoire of HLA-E reveals a binding motif that is strikingly similar to HLA-A2. *Mol Immunol* **53**, 126-31 (2013).
19. Weinzierl, A.O. et al. Features of TAP-independent MHC class I ligands revealed by quantitative mass spectrometry. *Eur J Immunol* **38**, 1503-10 (2008).
20. Oliveira, C.C. & van Hall, T. Importance of TAP-independent processing pathways. *Mol Immunol* **55**, 113-6 (2013).
21. Del Val, M., Iborra, S., Ramos, M. & Lazaro, S. Generation of MHC class I ligands in the secretory and vesicular pathways. *Cell Mol Life Sci* **68**, 1543-52 (2011).
22. Gil-Torregrosa, B.C., Raul Castano, A. & Del Val, M. Major histocompatibility complex class I viral antigen processing in the secretory pathway defined by the trans-Golgi network protease furin. *J Exp Med* **188**, 1105-16 (1998).
23. Medina, F. et al. Furin-processed antigens targeted to the secretory route elicit functional TAP1-/-CD8+ T lymphocytes in vivo. *J Immunol* **183**, 4639-47 (2009).
24. Martoglio, B. & Dobberstein, B. Signal sequences: more than just greasy peptides. *Trends Cell Biol* **8**, 410-5 (1998).
25. Weihofen, A. & Martoglio, B. Intramembrane-cleaving proteases: controlled liberation of proteins and bioactive peptides. *Trends Cell Biol* **13**, 71-8 (2003).
26. Durgeau, A. et al. Different expression levels of the TAP peptide transporter lead to recognition of different antigenic peptides by tumor-specific CTL. *J Immunol* **187**, 5532-9 (2011).
27. El Hage, F. et al. Preprocalcitonin signal peptide generates a cytotoxic T lymphocyte-defined tumor epitope processed by a proteasome-independent pathway. *Proc Natl Acad Sci U S A* **105**, 10119-24 (2008).
28. Oliveira, C.C. et al. Peptide transporter TAP mediates between competing antigen sources generating distinct surface MHC class I peptide repertoires. *Eur J Immunol* **41**, 3114-24 (2011).
29. Verweij, M.C. et al. Structural and functional analysis of the TAP-inhibiting UL49.5 proteins of varicelloviruses. *Mol Immunol* **48**, 2038-51 (2011).
30. Van Hall, T. et al. Differential influence on cytotoxic T-lymphocyte epitope presentation by controlled expression of either proteasome immunosubunits or PA28. *J. Exp. Med.* **192**, 483-494 (2000).
31. van Stipdonk, M.J. et al. Design of agonistic altered peptides for the robust induction of CTL directed towards H-2Db in complex with the melanoma-associated epitope gp100. *Cancer Res* **69**, 7784-92 (2009).
32. Riebeling, C., Allegood, J.C., Wang, E., Merrill, A.H., Jr. & Futerman, A.H. Two mammalian longevity assurance gene (LAG1) family members, trh1 and trh4, regulate dihydroceramide synthesis using different fatty acyl-CoA donors. *J. Biol. Chem.* **278**, 43452-9 (2003).
33. Yu, J. et al. JNK3 signaling pathway activates ceramide synthase leading to mitochondrial dysfunction. *J Biol Chem* **282**, 25940-9 (2007).

34. Golde, T.E., Wolfe, M.S. & Greenbaum, D.C. Signal peptide peptidases: a family of intramembrane-cleaving proteases that cleave type 2 transmembrane proteins. *Semin Cell Dev Biol* **20**, 225-30 (2009).
35. Weihofen, A. et al. Targeting presenilin-type aspartic protease signal peptide peptidase with gamma-secretase inhibitors. *J Biol Chem* **278**, 16528-33 (2003).
36. Weihofen, A., Lemberg, M.K., Ploegh, H.L., Bogyo, M. & Martoglio, B. Release of signal peptide fragments into the cytosol requires cleavage in the transmembrane region by a protease activity that is specifically blocked by a novel cysteine protease inhibitor. *J Biol Chem* **275**, 30951-6 (2000).
37. Martoglio, B. & Golde, T.E. Intramembrane-cleaving aspartic proteases and disease: presenilins, signal peptide peptidase and their homologs. *Hum Mol Genet* **12 Spec No 2**, R201-6 (2003).
38. Friedmann, E. et al. SPPL2a and SPPL2b promote intramembrane proteolysis of TNFalpha in activated dendritic cells to trigger IL-12 production. *Nat Cell Biol* **8**, 843-8 (2006).
39. Li, X. et al. Structure of a presenilin family intramembrane aspartate protease. *Nature* **493**, 56-61 (2013).
40. Fluhrer, R. et al. The alpha-helical content of the transmembrane domain of the British dementia protein-2 (Bri2) determines its processing by signal peptide peptidase-like 2b (SPPL2b). *J Biol Chem* **287**, 5156-63 (2012).
41. Lemberg, M.K. & Martoglio, B. Requirements for signal peptide peptidase-catalyzed intramembrane proteolysis. *Mol Cell* **10**, 735-44 (2002).
42. Lemberg, M.K. & Martoglio, B. On the mechanism of SPP-catalysed intramembrane proteolysis; conformational control of peptide bond hydrolysis in the plane of the membrane. *FEBS Lett* **564**, 213-8 (2004).
43. McLauchlan, J., Lemberg, M.K., Hope, G. & Martoglio, B. Intramembrane proteolysis promotes trafficking of hepatitis C virus core protein to lipid droplets. *EMBO J* **21**, 3980-8 (2002).
44. Loureiro, J. et al. Signal peptide peptidase is required for dislocation from the endoplasmic reticulum. *Nature* **441**, 894-7 (2006).
45. Schrul, B., Kapp, K., Sinning, I. & Dobberstein, B. Signal peptide peptidase (SPP) assembles with substrates and misfolded membrane proteins into distinct oligomeric complexes. *Biochem J* **427**, 523-34 (2010).
46. Snyder, H.L. et al. Two novel routes of transporter associated with antigen processing (TAP)-independent major histocompatibility complex class I antigen processing. *J. Exp. Med.* **186**, 1087-98 (1997).
47. Snyder, H.L., Bacik, I., Yewdell, J.W., Behrens, T.W. & Bennink, J.R. Promiscuous liberation of MHC-class I-binding peptides from the C termini of membrane and soluble proteins in the secretory pathway. *Eur. J. Immunol.* **28**, 1339-46 (1998).
48. Puente, X.S., Sanchez, L.M., Overall, C.M. & Lopez-Otin, C. Human and mouse proteases: a comparative genomic approach. *Nat Rev Genet* **4**, 544-58 (2003).
49. Kirkin, V. et al. The Fas ligand intracellular domain is released by ADAM10 and SPPL2a cleavage in T-cells. *Cell Death Differ* **14**, 1678-87 (2007).
50. Beisner, D.R. et al. The intramembrane protease Sppl2a is required for B cell and DC development and survival via cleavage of the invariant chain. *J Exp Med* **210**, 23-30 (2013).
51. Bergmann, H. et al. B cell survival, surface BCR and BAFFR expression, CD74 metabolism, and CD8- dendritic cells require the intramembrane endopeptidase SPPL2A. *J Exp Med* **210**, 31-40 (2013).
52. Schneppenheim, J. et al. The intramembrane protease SPPL2a promotes B cell development and controls endosomal traffic by cleavage of the invariant chain. *J Exp Med* **210**, 41-58 (2013).

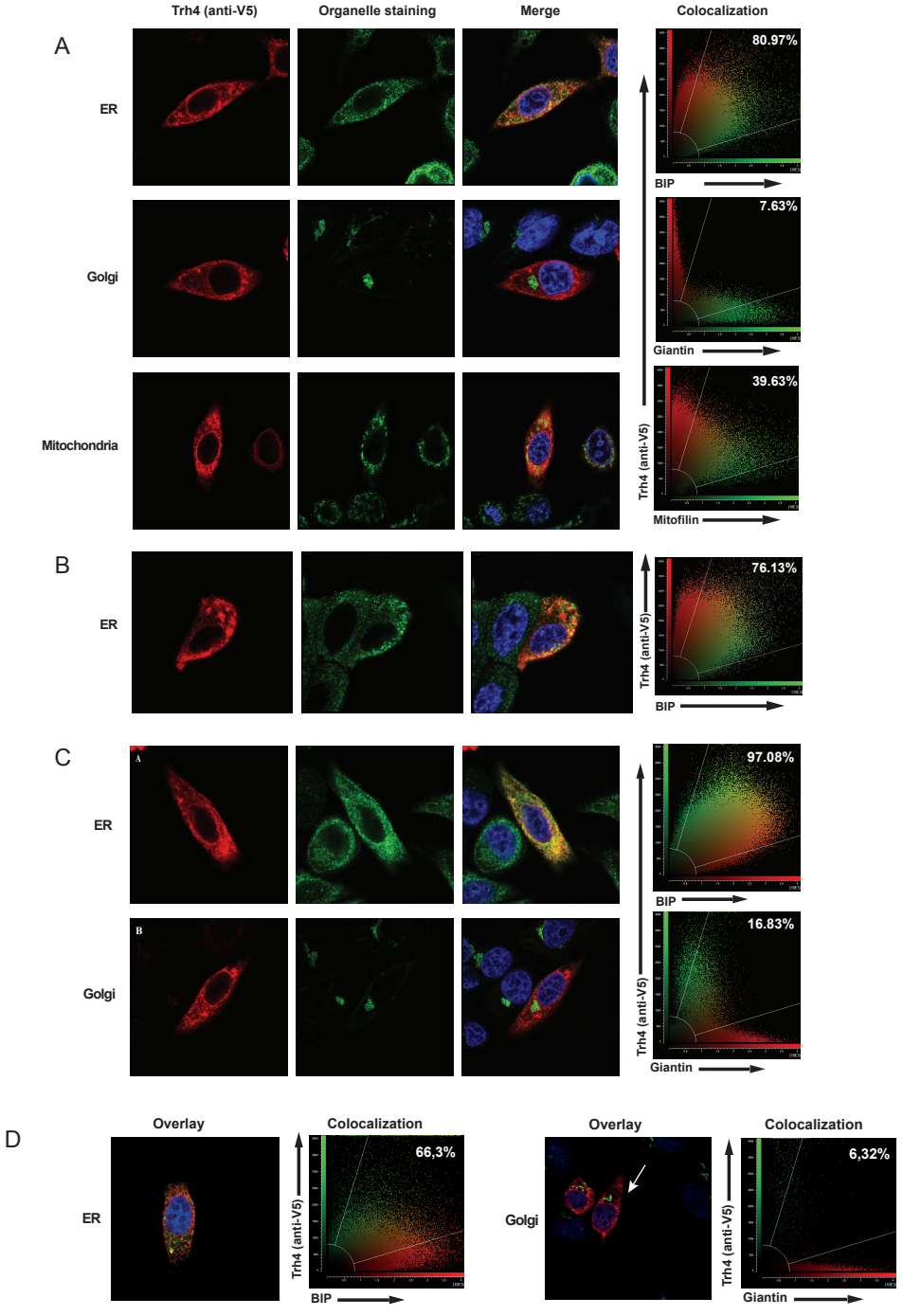
Trh4 (anti-V5)
Organelle staining
Merge
Colocalization
A
ER
Golgi
Mitochondria
80.97%
BIP
7.63%
Giantin
39.63%
Trh4 (anti-V5)
Mitofilin
B
ER
76.13%
Trh4 (anti-V5)
BIP
C
ER
Golgi
97.08%
BIP
16.83%
Trh4 (anti-V5)
Giantin
D
Overlay
Colocalization
ER
66,3%
Trh4 (anti-V5)
BIP
Overlay
Colocalization
Golgi
6,32%
Trh4 (anti-V5)
Giantin

◄ **Supplementary Figure 1. Trh4 localizes in the ER of TAP-proficient and TAP-deficient cells.** Confocal microscopy images were taken from transfected cells with V5-tagged Trh4 constructs. Cells were co-stained with antibodies against BIP (ER), giantin (golgi) and mitofilin (mitochondria). Computer-assisted analysis was performed using LAS AF software to calculate colocalization. At least ten images were included of two independent experiments. (A) HeLa cells transfected with the C-terminally tagged Trh4 construct. (B) TAP-deficient MCA cells with the N-terminally tagged Trh4 construct. (C) HeLa cells expressing the Trh4 construct lacking the first 32 amino acids (Del #1 construct from Fig 5A), which was predicted to constitute the leader sequence by the SignalP 4.1 Server (www.cbs.dtu.dk). V5 antibody tag was located at the C-terminus of this construct. (D) HeLa cells with a Trh4 construct in which the C-terminal amino acids 368-387, including the peptide-epitope, were removed and the V5 tag was introduced at the N-terminus.

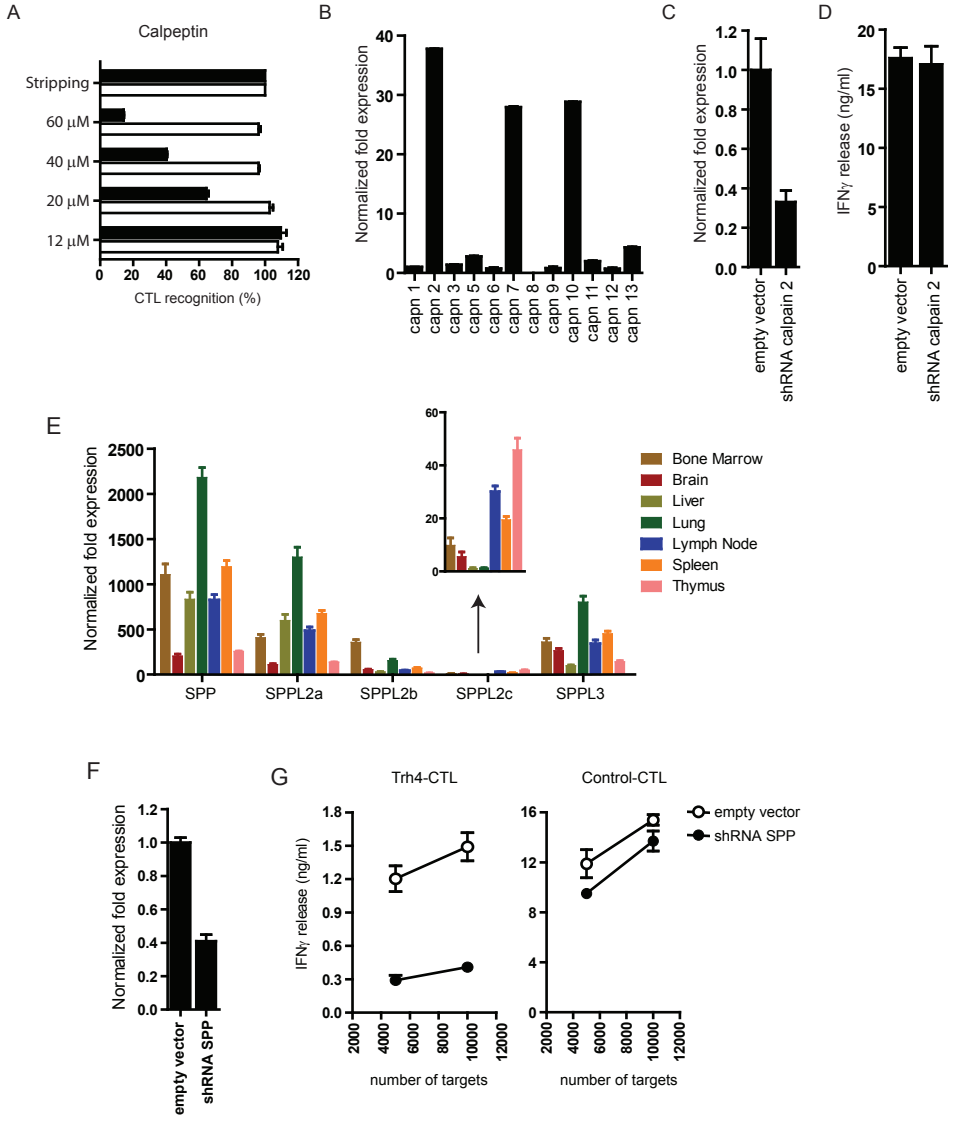

Supplementary Figure 2. Presentation of Trh4-derived peptide is not affected by calpain 2 silencing, but is SPP-dependent. (A) RMA-S cells were incubated with the protease inhibitor calpeptin at the indicated concentrations for 1h. Cells were washed and incubated with a mild acid solution to disrupt MHC-I/peptide complexes from the cell surface. After washing, cells were incubated again with calpeptin for additional 6h to allow recovery of MHC-I/peptide complexes and then incubated overnight with Trh4-specific CTL in the presence of Brefeldin A, to prevent release of IFN-γ. Intracellular cytokine staining was performed and percentage of activated CTL was determined by flow cytometry. Control CTL recognized the MuLV gag-leader peptide (CCLCLTVFL) on RMA cells. At the given calpeptin concentrations no toxicity on target cells was detected. (B) Expression of the calpain family member genes was analysed in RMA-S cells with qPCR. Expression levels were normalized to GAPDH housekeeping gene and expressed relative to the calpain 1 gene. Primer sequences are given in Suppl Table I. (C) RMA-S cells were transduced with lentiviruses encoding shRNA sequences that target calpain 2 or an ▶

- empty vector, leading to decreased mRNA levels of this gene. (D) CTL recognition of RMA-S cells with downregulated expression of calpain 2 was comparable to control RMA-S targets. Data are representative of three independent experiments. (E) Expression levels of SPP family members in mouse organs. RNA from complete mouse organs of wild type C57BL/6 mice was extracted and expression of SPP family members was determined by qPCR. Expression levels were normalized to GAPDH housekeeping gene and expressed relative to the SPPL2c sample in liver. (F) Silencing of SPP in TAP-deficient MCA cells was reached by lentivirus-mediated expression of shRNA constructs. Empty shRNA vector served as control. Efficiency of downregulated levels of transcripts was measured by qPCR. (G) Cells with silenced SPP were tested for recognition by Trh4-specific CTL or control CTL reactive to an independent K^b-presented peptide. Data are representative of three independent experiments.

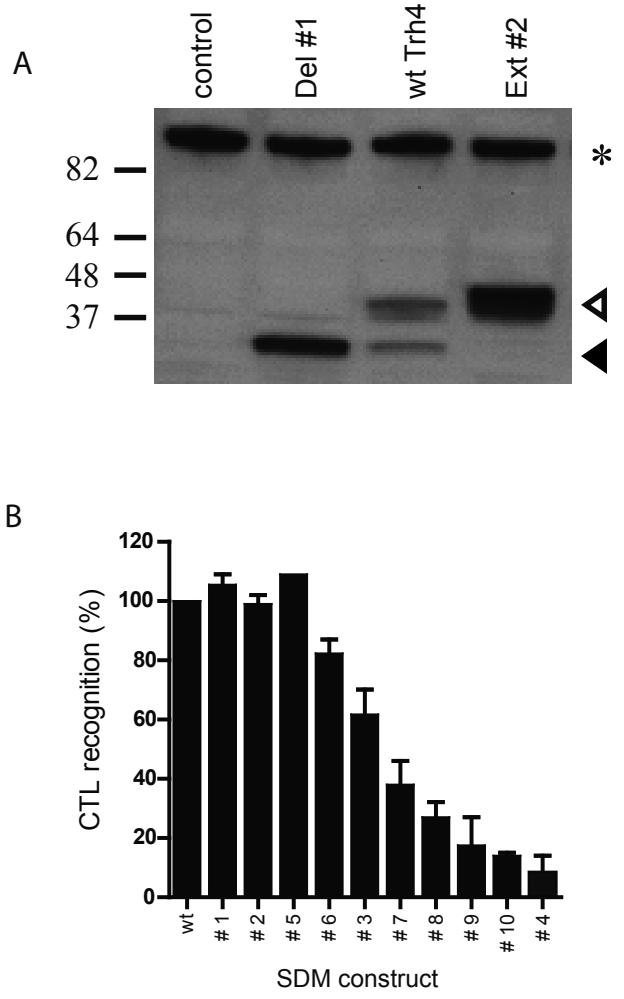

Supplementary Figure 3. Detection of V5-tagged Trh4 constructs by western blot and CTL recognition efficiency of all side-directed mutagenesis constructs. (A) HeLa cells were transiently transfected with V5-tagged Trh4 constructs. The tag was introduced at the N-terminus of the protein (at aa position 33; 'Del #1' and 'wt Trh4') or as an extension at the C-terminus ('Ext #2'), see Fig 5A. Two days later the cells were lysed and proteins were separated on SDS-page gel. Western blot analysis was performed with anti-V5 antibodies to confirm expression of these constructs after transfection. Data are representative of three independent experiments. Open triangle indicates full length Trh4 protein, closed triangle represents Trh4 without the first 32aa, predicted to be a leader sequence and * indicates a non-specific band present in all HeLa lysates, serving as loading control. (B) The Trh4 gene was mutated at single positions using site-directed mutagenesis. The construct numbers refer to the constructs mentioned in Figure 5C. These Trh4 constructs were transiently transfected into HeLa cells together with the mouse MHC-I molecule D^b. Two days later HeLa cells were collected and incubated at different target concentrations with Trh4-specific CTL. CTL recognition was determined by IFN-γ release in the supernatants and quantified by ELISA and the efficiency of CTL recognition was calculated as a percentage compared to the wild type construct using 'area under the curve' results of original line graphs (see Figure 5D). Depicted data are compiled from three independent experiments and means plus standard error of the means are plotted.

Supplementary Table 1. Primer sequences for the quantitative PCR for the mouse Calpain family.

Name	Gene ID	Forward primer (5'->3')	Reverse primer (5'->3')	Prod. Size (bp)
Calpain 1	12333	TTCTTCCATTCTTCCTCTG	CTTCCTTCCTGTTCTGAG	114
Calpain 2	12334	TTCGGCATCTATGAGGTT	CGGAGGTTAATGAAGGTATC	116
Calpain 3	12335	GAGGACTCTGAGGTAATCTG	GCGAAGCCAATAGTGAAG	101
Calpain 5	12337	CACTGACGAGGCTAAGAG	CTTGATGGAGGCACTGAT	85
Calpain 6	12338	GGAACTGACCTTGGACAT	TTCATTGGCATACTTCTTCTC	121
Calpain 7	12339	TACTCGGTGGCGGCTCTG	CTCATTGTCCTCCTCGTGTCCTATT	90
Calpain 8	170725	ACTACACCATCCAGAAGG	TCCAGTCACAGAGTATGC	131
Calpain 9	73647	GGACGGACACCTGAGTAG	CTGGAATCGCTCTGAGACT	97
Calpain 10	23830	AGTGGTATCTTCATTCCTTAGTG	TCTGCCTGCCTAGTGTAA	121
Calpain 11	268958	GGAGGTGAACAGCCATCT	AAGCAGGAAGTCAGCATCT	91
Calpain 12	60594	GCATATCCACATCTTCCA	CTTCATCATCGTCATCCT	143
Calpain 13	381122	GCTACTTGGCTCCTATTCC	GATTGCGGTCTTCACTGT	136